

Semi-active Control Study of Asymmetric MR-damper in Vehicle Suspension

Wang Enrong^{1, 2}, Ma Xiaoqing², Rakheja Subhash², Su Chunyi²

(College of Electrical & Electronic Engineering, Nanjing Normal University, 210042, Nanjing, PRC)

(Department of Mechanical & Industrial Engineering, Concordia University, H3G 1M8, Montreal, Canada)

Abstract: On the basis of the generalized asymmetric hysteresis model which has recently been proposed by the authors, this paper deals with semi-active control for the vehicle suspension vibration attenuation by employing a semi-actively controllable magnetorheological (MR) fluid damper. The proposed asymmetric model of an MR-damper is employed in a 2-DOF “quarter-car” model, and the “skyhook” control law is applied to implement variable damping deduced from the MR-damper. The simulation results demonstrate the contributions of damping asymmetry and hysteresis in response to the semi-active suspension, and suggest that the semi-active nonlinear controller synthesis can be greatly simplified to achieve superior vibration attenuation performance of the vehicle suspension.

Key words: magnetorheological fluid damper, asymmetric $f-v$ hysteresis model, semi-active control, “quarter-car” vehicle model

CLC number: TH703.62, **Document code:** B, **Article ID:** 1672-1292(2003)03-0001-07

1 Introduction

In order to satisfy the various conflicting performance requirements of automotive suspensions, a vast number of semi-active and active suspension systems have been explored to generate variable forces in accordance with the varying excitation and response variables^[1], and the vehicle suspensions are designed to provide highly asymmetric damping in compression and rebound to ensure adequate tire-road interactions. The studies on semi-active variable damping concepts using conventional hydraulic dampers have established that such dampers can effectively track the force that could be generated by a fully active force generator when the force is of dissipative nature, while the associated cost and hardware complexities are considerably lower^[2]. The semi-active controllable MR dampers have been commercially developed for vehicle suspension applications^[3]. However, the MR-dampers exhibit highly nonlinear variations in damping force attributed to the hysteresis and force-limiting property as functions of the intensity of the applied magnetic field, and displacement and velocity responses of the piston^[4], and the reported studies invariably consider damping properties that are symmetric in compression and rebound^[4-6].

In this study, a generalized asymmetric hysteresis model of the MR-damper, newly proposed by the authors in literatures^[7], is employed within a 2-DOF “quarter-car” model, and a sky-hook based semi-active controller is also applied to evaluate the system dynamic performance. The results show that the semi-active MR damper can yield considerably superior vibration attenuation performance for vehicle suspension, and the contributions due to hystere-

Receipt date: 2003-03-27.

Foundation Items: Supported by the Senior Visiting Scholarship of Chinese Scholarship Council (20H05002), the Natural Science Foundation of the Education Commission of Jiangsu Province (03KJB510072) and the Doctoral Scholarship of Concordia University in Canada.

Biographical Notes: Wang Enrong (1962), male, Ph. D graduate, associate professor, erwang@njnu.edu.cn, the interested researches are application study of semi-actively controllable magnetorheological fluid damper in vehicle suspension and projects corresponding to the discipline of electrical engineering & automation.

sis are further discussed.

2 Asymmetric Hysteresis Model

Figure 1 illustrates a schematic of an MR-damper, comprising electromagnetic coils and bleed orifices within the piston, and gas and hydraulic chambers within the cylinder that are separated by a diaphragm. The force versus velocity ($f-v$) characteristics of the MR-damper, asymmetric in compression and rebound corresponding to a specific control current, could be characterized by the generalized hysteresis loop depicted in Fig. 2. The damping characteristics, specifically the force-limiting nature and the magnitude of hysteresis, are strongly dependent upon the magnitude of the control current and the nature of vibration^[4]. The generalized asymmetric model was formulated as follows^[7].

$$f(v, i) = \begin{cases} \left(f_t \cdot \frac{1 - e^{-\alpha(v + v_h + v_d)}}{1 + e^{-\alpha(v + v_h + v_d)}} - f_d \right) \cdot (1 + k_{vc} \cdot |v|), & v \geq 0 \\ \left(f_t \cdot \frac{1 - e^{-\alpha(v + v_h + v_d)}}{1 + e^{-\alpha(v + v_h + v_d)}} - f_d \right) \cdot (1 + k_{ve} \cdot |v|), & v < 0 \end{cases} \quad (1)$$

where f stands for the interested damping force, and v_h is piston velocity corresponding to zero damping force

$$v_h = \text{sgn}(\dot{x}) \cdot k_4 \cdot v_m \cdot \left(1 + \frac{k_3}{1 + e^{-a_3(i + I_1)}} - \frac{k_3}{1 + e^{-a_3 \cdot I_1}} \right) \quad (2)$$

f_t refers to the transition force, taken as the mean value of f_p and f_{in} , which strongly depends upon the control current i and the peak velocity v_m

$$f_t = f_0 \cdot (1 + e^{a_1 \cdot v_m}) \cdot \left(1 + \frac{k_2}{1 + e^{-a_2 \cdot (i + I_0)}} - \frac{k_2}{1 + e^{-a_2 \cdot I_0}} \right) \quad (3)$$

The damping coefficients in compression and rebound, k_{vc} and k_{ve} are expressed as a function of the peak velocity v_m

$$k_{vc} = k_{1c} \cdot e^{-a_4 \cdot v_m} \text{ and } k_{ve} = k_{1e} \cdot e^{-a_4 \cdot v_m} \quad (4)$$

The parameters v_d and f_d define the asymmetry in terms of offset in the velocity and force axes, respectively

$$f_d = k_5 \cdot f_t \text{ and } v_d = k_6 \cdot v_m \quad (5)$$

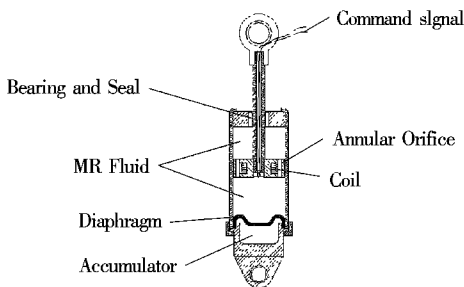


Fig. 1 Schematic of an MR-damper

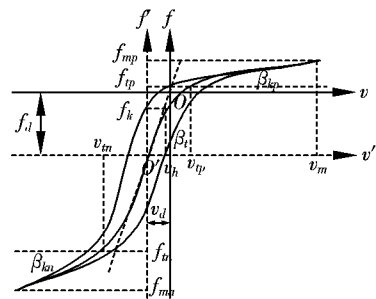


Fig. 2 A generalized asymmetric hysteresis loop

The model expressed in (1) ~ (5) requires identification of a total of 16 parameters ($a_0, a_1, a_2, a_3, a_4, I_0, I_1, f_0, k_0, k_{1c}, k_{1e}, k_2, k_3, k_4, k_5, k_6$) from the measured data, and can be easily simplified to yield mean asymmetric $f-v$ characteristics by letting $k_4=0$, and can be also reduced to characterize symmetric $f-v$ characteristics by letting $k_5=k_6=0$ and $k_{1c}=k_{1e}$. Furthermore, the peak velocity parameter v_m can be estimated from the instantaneous velocity, position and acceleration responses. For harmonic excitation and response, this parameter is obtained from^[4]

$$v_m = a_m \cdot \omega = \sqrt{(x\dot{)}^2 - \dot{x}\dot{x}} \tag{6}$$

where, x , $x\dot{}$ ($v = x\dot{}$) and \ddot{x} represent the relative displacement, velocity and acceleration of the piston, respectively.

A vehicle suspension, equipped with nonlinear and asymmetric MR-damper, however, may yield non-harmonic responses. Assuming that the damper exhibits hysteretic $f-v$ characteristics that are primarily dependent upon the fundamental harmonic component, Equation (6) could be effectively applied to estimate the value of v_m through application of a second order low-pass filter function, $H(s) = \frac{1}{(\omega_c^{-1}s + 1)^2}$, where ω_c is the cut-off frequency.

Herein, the measured $f-v$ data, acquired for a commercially available symmetric MR-damper under a wide range of control currents and excitation and response conditions, was considered for model parameter identification, and the asymmetric $f-v$ behavior was realized from the available data by introducing constant offsets in the force and velocity, such that the resulting data resulted in an asymmetry factor of about 4. The resulting asymmetric $f-v$ data is used to identify the model parameters expressed in (1) ~ (6), which are summarized in Table 1^[7].

Table 1 Model parameters identified from the measured data

Parameter	Value	Parameter	Value
a_0	1300	k_0	112.5
$a_1, (m/s)^{-1}$	1.75	k_{1c}	2.5
$a_2, (amp)^{-1}$	2.85	k_{1e}	5.2
$a_3, (amp)^{-1}$	1.55	k_2	19.4
$a_4, (m/s)^{-1}$	4.60	k_3	2.90
I_0, amp	0.05	k_4	0.095
I_1, amp	-0.08	k_5	0.65
f_0, N	17.9	k_6	0.12

Figure 3 shows a comparison of the model results with the measured data comprising the constant offsets. Figure 3(a) shows the computed results and measured data attained under 6.25 mm peak displacement excitation at a frequency of 5 Hz, while the current is varied from 0 up to 1.5 A. The results attained under constant current of 0.75 A and 6.25mm amplitude different frequencies are presented in Fig. 3(b). The results show reasonably good agreements between the model results and the measured data.

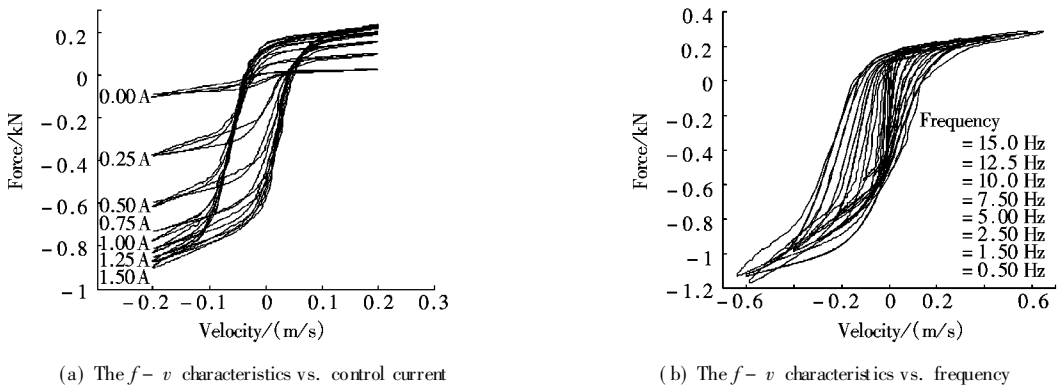


Fig. 3 Comparison of computed and measured $f-v$ characteristics of an asymmetric MR-damper (Simulation; measured)

3 Semi-active controller synthesis

The proposed model, formulated in (1) ~ (6), is applied in a 2-DOF “quarter-car” vehicle model as shown in Fig. 4 to study the behaviors of the dynamic system on the suspension performance. A skyhook control scheme^[1] is applied, on the basis of mean and hysteretic $f-v$ characteristics, to explore the influence of hysteresis on the per-

formance. The “quarter-car” model comprises a sprung mass m_s and unsprung mass m_u , and a suspension represented by a linear spring k_s and the damping force f expressed in (1). The tire is characterized by a linear spring k_t and viscous damping c_t with a point contact with the road. The motion equations of the system are written as

$$\begin{cases} m_s \ddot{x}_s + k_s(x_s - x_u) + f = 0 \\ m_u \ddot{x}_u + c_t(\dot{x}_u - \dot{x}_i) + k_t(x_u - x_i) - k_s(x_s - x_u) - f = 0 \end{cases} \quad (7)$$

where x_i denotes the displacement excitation at the tire-road interface, and x_s and x_u are the displacement responses of the sprung and unsprung masses, respectively. The relative velocity of the piston is defined as $v = \dot{x}_u - \dot{x}_s$ in the above-mentioned damping model. The damper undergoes compression when $\dot{x}_u - \dot{x}_s > 0$ and rebound motion when $\dot{x}_u - \dot{x}_s \leq 0$.

The quarter-car model is initially analyzed under sinusoidal excitations in the 0.5 to 20 Hz range with displacement magnitudes of 1.25 cm and 2.5 cm. The model parameters used are: $m_s = 288.9$ kg, $m_u = 28.6$ kg; $k_s = 19.96$ kN/m; $k_t = 155.9$ kN/m; and $c_t = 100$ N·s/m^[8]. A semi-active control policy, based upon the skyhook control, is formulated as follows

$$i = \begin{cases} k \cdot |\dot{x}_s|; & \dot{x}_s(\dot{x}_s - \dot{x}_u) \geq 0 \\ 0; & \dot{x}_s(\dot{x}_s - \dot{x}_u) < 0 \end{cases} \quad (8)$$

where k is an adjustable gain of the “skyhook” control law, and i is limited to 1.0 A.

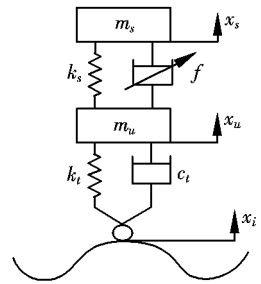


Fig 4 2-DOF “Quarter-car” model of the vehicle comprising the variable MR-damper

4 Results and Discussions

The simulations are performed using 0.25 Hz cut-off frequency in the low-pass filter and “skyhook” control gain of 7. Figure 5 shows the time-histories of the controller employing a semi-actively asymmetric MR-damper under selected excitation conditions. Fig. 5(a) illustrates control condition logic (on-off) corresponding to (4), while Fig. 5(b) shows the response of the control current. The control logic depends on the signs of the sprung mass velocity and the suspension relative velocity, which are illustrated in Fig. 6. The control logic, as shown in Fig. 5 (a), can be easily deduced from Fig. 6 in subject to the condition of (4).

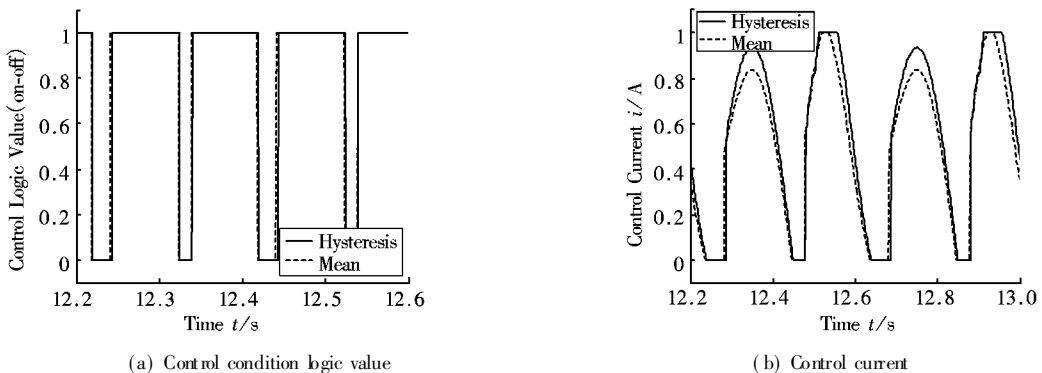


Fig. 5 Comparison of control values with mean and hysteric

The effect of damping hysteresis on the semi-active suspension response is investigated by comparing the sprung mass velocity and the suspension relative velocity of the system with those attained using the mean damping curve in Fig. 6. The results show that the damping hysteresis yields considerable peak noise shoot at specific instants in the response. This is caused by the control logic turning from off to on and the hysteresis effect at the time of relative velocity being cross over the zero-velocity critical point. Furthermore, the unsmoothness of responses are caused by

the nonlinearities of system owing to the semi-active nonlinear controller, and the damping force saturation, control current saturation and the hysteresis of the MR-damper.

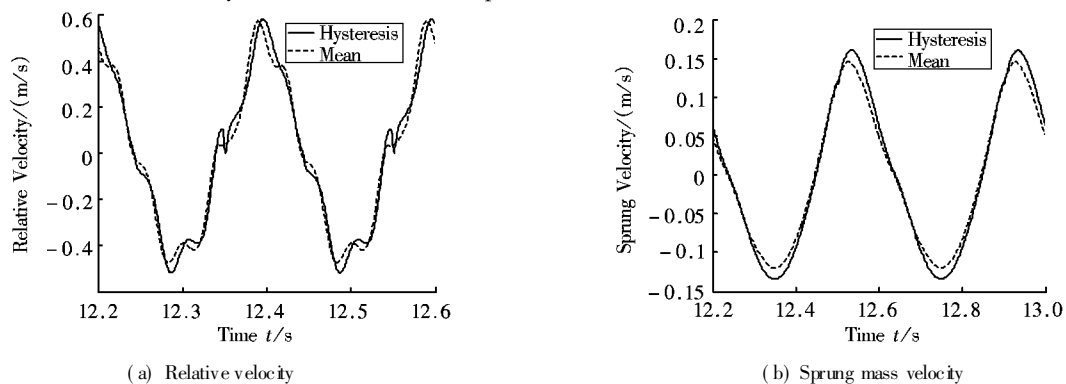


Fig. 6 Comparison of responses with mean and hysteretic damping

The model synthesis employed in the simulation utilizes the estimation of peak velocity v_m using the proposed filtering methodology. Figure 7(a) illustrates a comparison of v_m derived from (6) with that estimated using the low-pass filter. The results are shown corresponding to an excitation frequency of 2.5 Hz and peak amplitude of 2.5 cm. It is evident that the velocity response attained without the filter yields considerable random noise that is attributed to the hysteresis and the force limiting properties of the MR damper, while the use of filter yields mean value of v_m . The results clearly show that the filter function can effectively estimate the peak velocity response. The use of the filter function yields insignificant influence on the system response as evident from the sprung mass displacement response shown in Fig. 6(b).

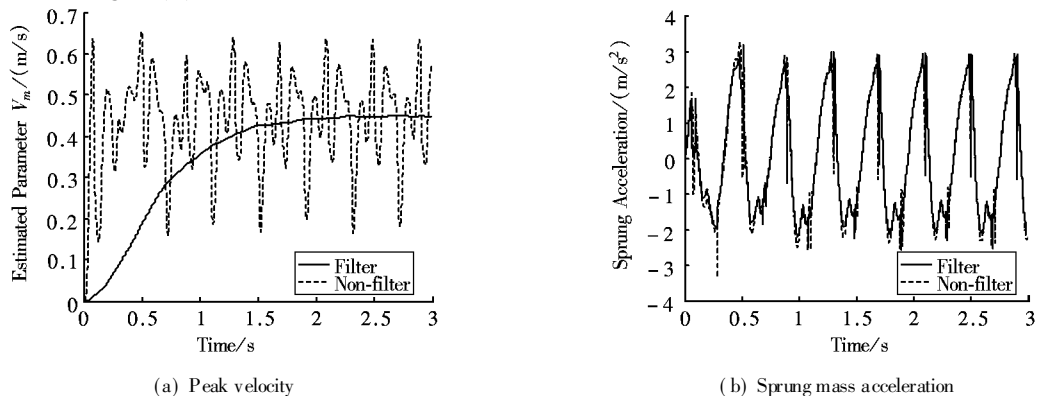


Fig. 7 Comparison of the peak velocity and the sprung mass acceleration responses of the model with and without the filter

Figure 8 reveals the effects of skyhook control gain on responses of the sprung mass acceleration and control current. The results show the comparison of responses in a smaller gain ($k=3$) with those in a larger gain ($k=7$). The use of a smaller gain can partly reduce the above-discussed peak noise shoot caused by hysteresis and on-off control logic, and economizes the input power requirement, but it may yield poor suspension performance due to limited damping force.

Figure 9 shows the acceleration transmissibility responses of the sprung mass of the quarter-vehicle model employing passive (open-loop; $i=0.2$ A and 0.5 A) and semi-active (closed-loop) damping, both being hysteretic. Owing to the downward shift in the displacement response^[9], attributed to damping asymmetry, the mean transmissibility magnitudes are evaluated from the peak-peak response magnitudes. The results clearly show that the skyhook-based semi-active control effectively suppresses the sprung mass resonant responses (around 1.2 Hz and 10.5

Hz), and yields superior vibration isolation. The results further illustrate that the MR-damper is an ideal semi-active controllable actuator. The transmissibility tends better with the increase of control current even in the open-loop system.

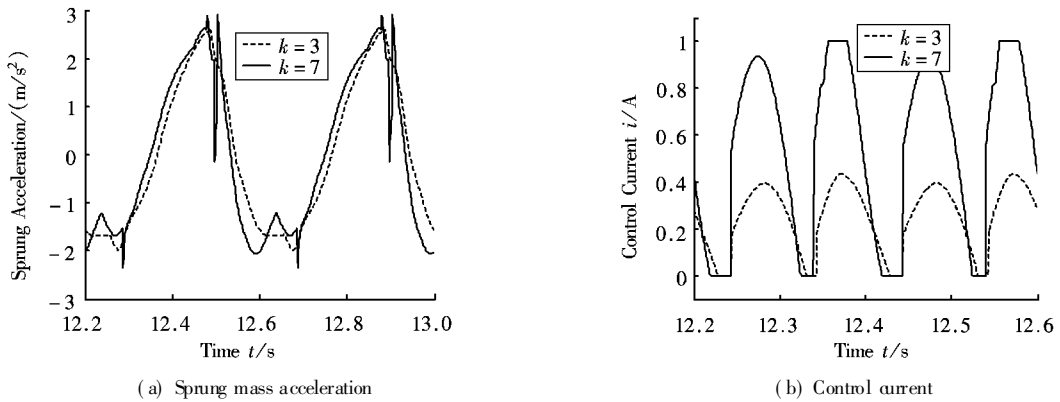


Fig. 8 Influence of control gain on the sprung mass acceleration and the control current

5 Conclusions

An analysis is performed on a quarter-vehicle model in conjunction with the skyhook semi-active control of an asymmetric and hysteretic MR damper. The effects of damper asymmetry and hysteresis on the response characteristics are investigated as a function of the control gain. An estimation methodology based upon the use of a low-pass filter is proposed to estimate the peak velocity response as required for the model synthesis, and the results show a reasonably good estimation of the mean peak velocity without altering the system response. The results further suggest that the semi-active MR damper can yield considerably superior vibration isolation performance of the vehicle suspension, and the contributions due to hysteresis could be greatly reduced by selecting lower values of the skyhook control gain.

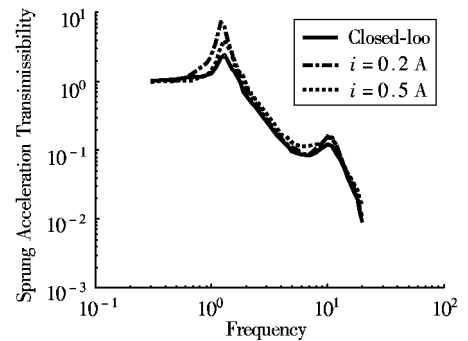


Fig. 9 Comparison of sprung acceleration transmissibilities of the open and closed systems

[References]

[1] Hwang S H, Heo S J, Kim H S, et al. Vehicle dynamic analysis and evaluation of continuously controlled semi-active suspensions using hardware-in-the-loop simulation[J]. *J of Vehicle System Dynamics*, 1997, 27: 423~ 434.

[2] Rakheja S, Woodroffe J. Role of suspension damping in enhancement of road friendliness of heavy vehicles[J]. *Heavy Vehicle System, Int J of Vehicle Design*, 1996, 3 (1~ 4): 363~ 381.

[3] Choi, S B, Suh M S, Park D W, et al. Neuro-fuzzy control of a tracked vehicle featuring semi-active electro-rheological suspension units[J]. *J of Vehicle Systems Dynamics*, 2001, 35(3): 141~ 162.

[4] Wang E R, Ma X Q, Rakheja S, et al. Modeling hysteretic characteristics of an MR fluid damper[J]. *Proc. of the Inst. of Mech. Engrs, Part D J. of Automobile Engineering*, Paper No. D05302/RV2 (to appear), 2003.

[5] Dyke S J, Spencer Jr B F, Sain M K, et al. Modeling and control of magnetorheological dampers for seismic response reduction [J]. *J of Smart Materials and Structures*, 1996, 5(5): 565~ 575.

[6] Wereley N M, Pang L, Kamath G M. Idealized hysteresis modeling of electro-rheological and magneto-rheological dampers[J]. *J of Intelligent Material Systems and Structures*, 1998, 9: 642~ 649.

- [7] Wang E R, Ma X Q, Rakheja S, et al. A General Model of an MR-fluid damper[A] . *Proc. of Int. 9th Conference On Sound And Vibration*[C] . July 8~ 11, Orlando, USA, 2002.
- [8] Thompson A G, Davis B R. Technical Note: Force control in electrohydraulic active suspension revised[J] . *J of Vehicle System Dynamics*, 2001, 35(3): 217~ 222.
- [9] Warner B. Analytical and experimental investigation of high performance suspension damper[D] . PH. D. Thesis, Concordia University, Montreal, Canada, 1996.

不对称磁流液阻尼器在汽车减振中的半主动控制

王恩荣^{1, 2}, 马晓青², 萨巴契·喏凯甲², 苏春翌²

(南京师范大学 电气与电子工程学院, 210042, 南京)

(康考迪亚大学 机械与工业工程系, H3G 1M8, 蒙特利尔, 加拿大)

[摘要] 根据作者新近提出的一种通用不对称滞环特性模型, 本文对磁流液(MR) 阻尼器在汽车减振应用进行了半主动控制研究. 将所提出的 MR 阻尼器不对称滞环模型应用在二自由度“四分之一”汽车模型, 并用“空挂”控制律来实现对 MR 阻尼器阻尼力的自动调节. 仿真结果验证了阻尼力不对称性和滞环特性对汽车悬挂性能的影响, 且表明所设计的半主动非线性控制器的复杂性大大减化, 并达到理想的汽车悬挂减振性能.

[关键词] 磁流液阻尼器, 不对称滞环模型, 半主动控制, “四分之一”汽车模型

[责任编辑: 刘健]